

PHYTO-ASSISTED SYNTHESIS OF SILVER NANOPARTICLES (AgNPs), CHARACTERIZATION, AND SCREENING THEIR ANTIMICROBIAL ACTIVITIES

Aiman Parveen^{1*}, Farheen Ezhar², Meenal Rehman³ and Azhar U. Khan³

¹Botany Section, Mayfair College, Moradabad, U.P., India

²Special Centre for Molecular Medicine, Jawaharlal Nehru University, New Delhi

³School of Basic Sciences, Department of Chemistry, Jaipur National University, Jaipur, Rajasthan, 302017, India

*Corresponding author*E-mail: draimanparveen@gmail.com

Abstract

The present study aims to develop a cost-effective and eco-friendly method for synthesizing silver nanoparticles (AgNPs) using *Alstonia* sp. leaf extract. The AgNPs were characterized using various physicochemical techniques, including Scanning electron microscopy (SEM), Transmission electron microscopy (TEM), and UV-visible spectroscopy. The UV-visible spectroscopy analysis revealed maximum absorption at 440 nm, which is a characteristic of AgNPs surface plasmon resonance. Transmission electron microscopy (TEM) and SEM confirmed the spherical shape of the nanoparticles, with an average diameter of 20 nm. Dynamic Light Scattering and zeta potential measurements were conducted on the fabricated AgNPs. The zeta potential was determined to be -34.7 mV, indicating the stability of the nanoparticles due to their strong negative surface charge. In vitro studies using Petri plates evaluated the antifungal, antibacterial, and nematicidal properties of biofabricated silver nanoparticles (AgNPs) against *Aspergillus flavus*, *Mycobacterium tuberculosis* and *Meloidogyne incognita*. At a concentration of 500 µg/mL, the AgNPs exhibited significant antifungal, antibacterial, and nematicidal activity. The synthesized AgNPs at 500 µg/ml showed 6% J2 juvenile mortality after 24h, 16% after 48h, and 29% after 72h. Around 58% reduction in hatching has been reported after 72h. 40-50% reduction in fungal growth at 500 µg/mL AgNPs treatment, and a strong inhibition zone occurs in the petriplate that shows the antibacterial activity of the synthesized nanoparticles.

Keywords: *Aspergillus flavus*, *Meloidogyne incognita*, *Mycobacterium tuberculosis*, AgNPs, *Alstonia* sp.

1. Introduction

Green nanotechnology has attracted much attention in recent years as researchers seek sustainable and environmentally friendly alternative methods for nanoparticle synthesis. The development of these technologies has shifted toward using biological sources for nanoparticle synthesis, aiming to minimize environmental impact by avoiding the use of toxic chemicals typically used in traditional methods. The biosynthesis of nanoparticles has been explored using various biological materials, including plants, bacteria, fungi, and algae. These methods provide an environmentally friendly approach and offer cost-effective and scalable production techniques for various nanoparticles such as Ag, Au, ZnO, CuO, and Fe₃O₄ (1). This shift towards green synthesis is in line with the broader goals of environmental sustainability and the circular economy, where agricultural waste and by-products are increasingly being utilized to produce valuable nanomaterials. Among the different bio sources used for nanoparticle synthesis, plant extracts have emerged as promising agents due to their rich content of phytochemicals that can act as reducing and stabilizing agents. For example, onion peel, olive leaves, and garlic peel extracts have been effectively used to synthesize silver and chromium oxide nanoparticles with significant antibacterial properties (2-6). Furthermore, plant-based nanoparticles have demonstrated enhanced biological activities, such as antimicrobial, antifungal, and photocatalytic effects, making them suitable for various applications, including wastewater treatment and biological control. The synthesis of AgNPs using environmentally benign plant extracts not only reduces reliance on hazardous chemicals but also opens new avenues for sustainable nanotechnology applications (3,6,7). Since agriculture is the cornerstone of a flourishing civilization, it must be preserved for future generations. The sustainable growth of agriculture is now the major priority. In 2020, the global agrochemical consumption is anticipated to be 50 x 10⁶ t for fertilizers based on phosphate, 120 x 10⁶ t for fertilizers based on nitrogen, and about 2.6 x 10⁶ t for insecticides (1,2). Conventional agricultural practices often overapply agrochemicals (fertilizers and insecticides) to crops in an attempt to maximize crop yields. Presently, over 50% of applied N and 85% of applied P are not reaching their intended targets, while less than 10% of applied insecticides do so (3,4). Pest attacks damage 20–40% of agricultural products worldwide, with plant diseases accounting for 16% of production loss (4,8).

The filamentous fungus *Aspergillus flavus* is a pathogenic and saprophytic fungus that produces aflatoxins causing disease in crops such as maize, cotton seeds, and peanuts, reducing crop yield (9). In addition, this fungus causes intoxication in humans by the consumption of nuts, grains, and their derived products contaminated by the fungus. Due to *A. flavus* infection the important crops and aflatoxin in grains, this contamination causes high losses in agriculture, so that hundreds of millions of dollars are lost to the U.S. and world economy annually (10). *Aspergillus* sp., causes disease in humans also. *Mycobacterium tuberculosis* causes tuberculosis in humans.

Plant parasitic nematodes result in significant agricultural losses, ranging from approximately \$US80 billion to \$US157 billion globally. *Meloidogyne incognita*, a plant parasitic nematode, is the causal organism behind root-knot disease in numerous significant crop plants, including peppers, tomatoes, lettuces, and so forth (11,12).

A number of suppressive techniques have been employed to reduce the harm that pests and pathogens cause. Many countries banned specific crops to prevent the spread of disease. Many chemical, biological, and other integrated pest management approaches are employed to increase the crop yield. Despite this, diseases still severely reduce agricultural productivity. Crop growth can be improved in agriculture by using nanoparticles. Non-metals, metallic oxides, metalloids, and carbon nanomaterials are NPs that have been demonstrated to prevent plant diseases. Copper, iron, titanium oxide, gold, silver, zinc oxide, and titanium dioxide are the most often studied and used NPs (13). The most frequently synthesized NPs are AgNPs, and, owing to their extensive and unique range of applications in medicine and agriculture, AgNPs have attracted the attention of academics as well as sparked a global boom of interest among experts in other fields. However, by promoting antibacterial action, AgNPs prevent resistance development. These characteristics make them safe alternatives to synthetic fungicides in the management of plant diseases. In contrast to chemically synthesized nanomaterials, biological nanomaterials have demonstrated high antibacterial activity against various diseases (14).

Biologically-synthesized AgNPs may have numerous uses, and they are simple, safe, dependable, biocompatible, and affordable (15,16). Biological methods, such as synthesis using plants, bacteria, and fungi, are gaining popularity because they are low-cost, simple to manage, employ mild reaction conditions across a range of hosts, and yield stable nanoparticles with controlled dimensions (17,18,19). Antimicrobial drugs, bio-labeling, sensors, filters, microelectronics, and catalysis are just a few of the many applications for silver nanoparticles (14,20). The growth of bacteria, fungi, viruses, and other microorganisms is inhibited by silver nanoparticles (AgNPs) (17,21,22).

Plants are rich in vitamins, minerals, and essential fatty acids and have bioactive compounds showing antimicrobial and antioxidant activities (23). Due to these properties, we chose this plant as a source for preparing AgNPs. In previous studies, silver nanoparticles were synthesized using an aqueous leaf extract of *Trigonella foenum-graecum* (24), seed extract of corn (25), and fungi (17).

Comparing green manufacturing of nanoparticles to conventional chemical and physical approaches reveals several benefits. It encourages environmental sustainability and biocompatibility for pharmaceutical and biomedical applications by doing away with the use of hazardous chemicals. Green synthesis, in contrast to conventional procedures, eliminates the possibility of harmful compounds being absorbed onto the surface of nanoparticles, which could have unfavorable impacts on medical applications. Green synthesis is also economical, scalable, and energy-efficient because it doesn't call for hazardous chemicals, high pressure, or temperatures (24,25).

In this context, the present study explores the green synthesis of silver nanoparticles (AgNPs) using *Alstonia* sp. leaf extract. By employing a simple and sustainable method, the synthesized AgNPs were thoroughly characterized using various physicochemical techniques. This study also investigates the antifungal, antibacterial, and nematicidal

properties of biofabricated AgNPs against *A. flavus*, *M. tuberculosis*, and the root-knot nematode *M. incognita* respectively. The findings contribute to the growing body of research on plant-based nanoparticles synthesis and highlight their potential as effective microbial control agents.

2. Materials and Methods

2.1. Biosynthesis of silver nanoparticles

For the green fabrication of AgNPs, the leaf extract of *Alstonia* sp. was used. Leaves were picked and washed numerous times with distilled water to remove dust, followed by drying at room temperature. The 10 g of leaves were cut into small pieces, put into 100 ml of distilled water, and boiled for 20 min on a hot plate. The solution was allowed to cool before filtering through Whatman filter paper, and the filtrate was then used to produce AgNPs. To synthesize green AgNPs, 20 ml of leaf filtrate was mixed with 80 ml of a 1 mM AgNO₃ solution, which was kept at room temperature while the color change was monitored. Once the color of the solution had fully formed after 24 hours, it was centrifuged for 15 minutes at 9000 rpm. To acquire AgNPs in powder form, the pellet was collected, cleaned, and dried using a freeze-dryer, while the supernatant was discarded. The antifungal activity and characterization of the powdered AgNPs were performed as described in previous research work (24,25).

2.2. Characterization of biosynthesized silver nanoparticles

2.2.1 Ultraviolet-visible spectrophotometer analysis

The formation of the reduced silver nanoparticles in colloidal solution was monitored by using a UV-vis spectrophotometer. The absorption spectra of the supernatants were taken between 200 and 800 nm, using a UV-vis spectrophotometer. The deionized water was used as the blank.

2.2.2 Scanning Electron Microscopy (SEM) and Transmission Electron Microscopy (TEM)

After an aqueous AgNPs drop was dried on the carbon-coated copper, SEM and TEM analyses were conducted. Samples for SEM and TEM grids were vacuum-sealed and dried in desiccators before being placed on a specimen holder. The size distribution and particle shape of the biosynthesized AgNPs were assessed.

2.2.3. Dynamic Light Scattering (DLS) and Zeta potential

The size distribution (hydrodynamic diameter) and surface charge of the fabricated AgNPs were analysed using dynamic light scattering (DLS) and zeta potential measurements, respectively, with a Litesizer 500 instrument.

2.3. Isolation and identification of fungal pathogen

Aspergillus flavus was cultivated on Potato Dextrose Agar (PDA) medium to cause sporulation (Figure 1). The PDA was placed in the laminar flow unit after being poured into Petri plates. To allow the fungus to mature, infected plant sections were moved to plates containing PDA and kept for five to seven days at 27±2°C. Pure isolates were identified on a morphological basis, such as colony and mycelium color, spore color, and size. Cultural characteristics such as colony color, shape, and margin were recorded by visual observation of fully covered *A. flavus*. Petri plates on a PDA were incubated at 27±2°C (17).

2.4. In vitro Petri plate assay for antifungal activity

Synthesized AgNPs were used to screen for the *in vitro* antifungal activities against plant pathogenic fungus *A. flavus*. For screening the antifungal activities, potato dextrose agar medium mixed with 500µg/ml AgNPs was used to screen the effect of AgNPs on mycelium growth of *A. flavus* compared with the control (without AgNPs) (17). The PDA medium was poured into 90×15 mm Petri plates and incubated for 7 days. On control plates, no treatment was given. Following incubation, 7mm diameter agar plugs containing fungus were placed concurrently in the middle of each Petri plate and allowed to incubate at 27±2°C. Following a fortnight of incubation, the radial expansion of the colony was measured. The test was performed three times. The percentage of inhibition (%) was calculated using the following formula:

$$\text{Inhibition rate (\%)} = \frac{C - T}{C} \times 100$$

Where C is the radial growth of the fungal pathogen in the control plate and T is the radial growth of the fungal pathogen in AgNPs-treated plates.

2.5. Antibacterial Analysis

The standard well-cutting and time-kill assay techniques were used to evaluate the antibacterial activity of the produced silver nanoparticles. The culture of the tuberculosis bacterium *M. tuberculosis* was obtained from the Special Centre for Molecular Medicine, Jawaharlal Nehru University, New Delhi. Before being incubated with nanoparticles, the bacterium was cultivated in 5 mL of Nutrient Broth (HiMedia) in a shaker at 35°C and 150 rpm until the culture reached an OD600 nm by 1.0, which corresponds to 10⁸ CFU ml⁻¹. *M. tuberculosis* was mixed with sterile distilled water and inoculated on Petri plates. The bacteria were then incubated at 35°C for 5 days and after incubation, growth was observed.

2.6. Isolation of root-knot nematode

The root-knot nematode, *M. incognita*, was isolated from afflicted eggplant roots. Sterilized forceps were used to pick egg masses, which were then placed in sieves at 25 ± 1°C for hatching. For inoculation, second-stage juveniles (J2) were selected (Figure 1).

2.7. Propagation of *Meloidogyne incognita*

The root-knot nematode *M. incognita* was isolated from infected eggplant roots and maintained in a greenhouse for research purposes. Egg masses were hand-picked with the help of sterilized forceps from infected roots. The isolated egg masses were washed with distilled water and placed in a small sieve of 9 cm diameter with 1mm pore size

containing layers of tissue paper. The sieve was placed in a Petri plate containing distilled water deep enough to contact the egg masses and these assemblies were kept in an incubator at $25 \pm 1^{\circ}\text{C}$ for the hatching of second-stage juveniles (J2). Hatched J2 were collected (Figure 1).

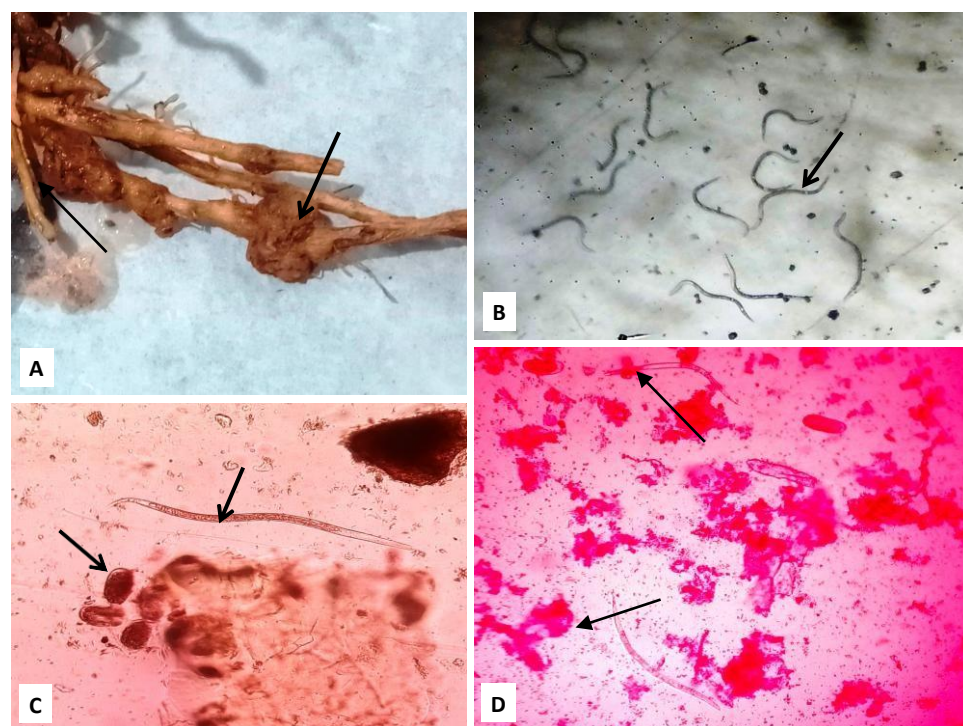


Figure 1. Figure of disease symptoms caused by the root-knot nematode *M. incognita*: (A) Large root knots at the root system of eggplants infected by *M. incognita*. (B) J2 Juveniles. (C) & (D) J2 Juveniles and Eggs stained with acid fuchsine.

2.8. Screening of the toxic effect of AgNPs on J2 juveniles of root-knot nematode bioassay

To ascertain the impact of AgNPs on *M. incognita* mortality, we took and filled each Petri plate with a 20 ml suspension in which 5 ml 500 $\mu\text{g}/\text{ml}$ suspension of AgNPs was mixed with 15 mL of distilled water. In each Petri plate, 100 newly hatched J2 were placed. At $25 \pm 1^{\circ}\text{C}$, the plates having a solution of nematodes and AgNPs were allowed to incubate for 24h, 48h, and 72h intervals, and during this time change in mortality was observed.

2.9. Egg hatching assay

To perform the hatching assay, each Petri plate had a volume of 20 ml and was filled with a 5 ml suspension containing 500 $\mu\text{g}/\text{ml}$ AgNPs, which was combined with 15 ml of distilled water. Each Petri plate contained five egg masses. As a control, a Petri plate was taken containing five egg masses along with 20 mL of double-distilled water. The effect on nematode hatching was determined for 24h, 48h, and 72h under the microscope. Juveniles that hatch from eggs were counted.

3. Results

3.1. Nanomaterials Characterization

UV-visible spectrum analysis was conducted using a Shimadzu UV-visible spectrophotometer (UV-1800, Japan) with a resolution of 1 nm between 200 and 800 nm. The synthesis and stability of AgNPs were confirmed through UV-Vis spectroscopy. The UV-Vis spectra of the biosynthesized AgNPs were recorded at ~ 440 nm and at various time intervals. The formation of AgNPs was validated by UV-Vis absorption spectroscopy using an aqueous leaf extract of *Alstonia* sp. The stability and green synthesis of the AgNPs were also verified using UV-Vis spectroscopy. It was observed that the production of stable AgNPs caused the greenish-brown solution containing leaf extract and AgNO₃ to turn yellowish-brown within 30 minutes. The UV-Vis spectra of the synthesized AgNPs are presented in Figure 2. The surface plasmon resonance (SPR) absorption band observed is attributed to the excitation of free electrons in the outermost orbitals of the AgNPs (17,26,27). The bioreduction of Ag⁺ and the creation of AgNPs may be caused by the presence of flavonoids and other phenolic groups. As a result, aqueous leaf extract demonstrates its dual function as a stabilizing and green-reducing agent (24,25,28).

3.3. Scanning Electron Microscopy (SEM) and Transmission Electron Microscopy (TEM) Analysis

SEM and TEM analyses were used to look at the size and shape of the synthesized AgNPs. The produced AgNPs, which were almost spherical, evenly sized, less aggregated, and well crystalline, are depicted in Figure 3a's SEM image. The AgNPs were around 20 nm in size. The spectrum (Figure 2) reveals a prominent peak indicative of the successful synthesis of silver nanoparticles. The elemental composition of the nanoparticles is approximately 55.2% silver by weight and 31.2% oxygen by weight. A minor nitrogen peak is also observed at around 0.2 keV, corresponding to a weight percentage of 13.6%. This suggests that although nitrogen-containing organic compounds

might have been involved in the nanoparticle formation, their incorporation into the final product was minimal. The low intensity of the nitrogen peak compared to the silver peak further supports the notion that the organic content within the nanoparticles is relatively low. Nevertheless, the presence of even trace amounts of nitrogen confirms the biogenic nature of the silver nanoparticles and the role of the leaf extract in their synthesis. The produced AgNPs are confirmed to be of nanoscale by transmission electron microscopy (TEM) (Figure 3b), with the majority of the particles having a spherical form and an average diameter of 20 nm. It shows that the silver nanoparticles are mostly spherical and evenly distributed, and are homogeneous. Because the AgNPs were encapsulated in the *Alstonia* sp. leaf extract, agglomeration of the AgNPs was not observed. The naturally occurring alkaloids, flavonoids, polyphenols, etc., in this plant are responsible for the encapsulation.

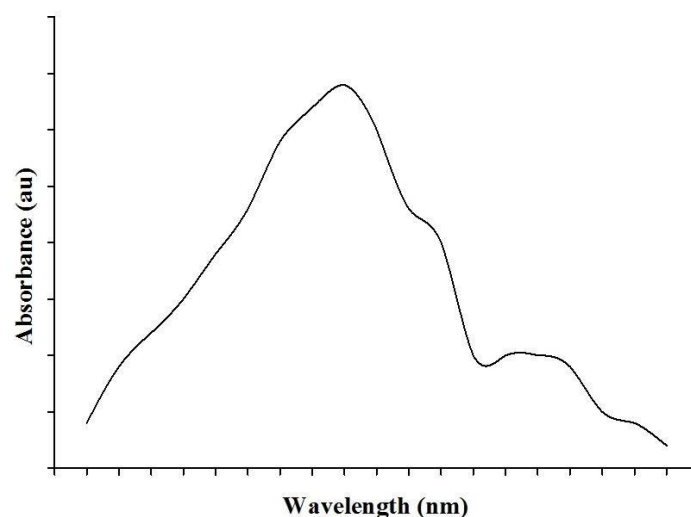


Figure 2. UV-visible spectra of biosynthesized AgNPs

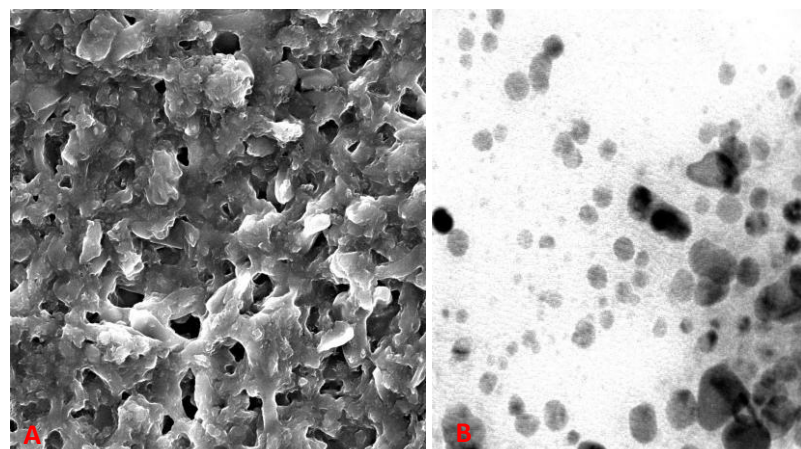


Figure 3. (a) Scanning electron microscopy (SEM) image, (b) TEM image of synthesized AgNPs

3.4. In vitro antifungal and antibacterial activity of biosynthesized AgNPs

Synthesized AgNPs were tested against the pathogenic fungi *A. flavus* and bacterium *M. tuberculosis*. In vitro study showed that AgNPs comprehensively inhibited the mycelial growth of the fungi *A. flavus*. The growth of *A. flavus* was considerably reduced to 40–50% (Figure 4,5,6) in potato dextrose medium with 500 µg/mL AgNPs compared with the control (without NPs) experiment. The bactericidal activity of AgNPs has been observed with respect to the concentrations used. AgNPs was found to be effective against mycobacterial strains. The presence of a strong inhibition zone shows the antibacterial activity of AgNPs (Figure 7). Microscopic and SEM studies showed that fungal mycelium and the tested bacterium was disturbed by synthesized AgNPs (Figures 6 & 8). In previous studies, we reported the antifungal and antibacterial activity of biosynthesized silver nanoparticles (17,24,44).

AgNPs were synthesized from plant *T. foenum-graecum* and also found antifungal and antibacterial efficacy against plant-pathogenic bacteria *Pseudomonas syringae* and plant-pathogenic fungus *Alternaria alternata* (24). According to the assay results, *P. syringae* and *A. alternata* were suppressed in the corresponding medium at 100 ppm of AgNPs. AgNPs have been shown to exhibit antifungal action against *Aspergillus* fungus species, according to Bocateet al. (34). According to Bahrami-Teimoori et al. (35), AgNPs exhibit antifungal action against *Macrophomina phaseolina*, *Alternaria alternata*, and *Fusarium oxysporum*. Fungal hyphae and conidial germination of fungus are negatively impacted by using silver nanoparticles as antimicrobial agents (36,37,34). Mishra et al. (38) produced silver nanoparticles using the supernatant of a bacterium culture that is vital to agriculture, *Serratia* sp. BHU-S4, and they highlighted the significance of this bacterium in controlling wheat spot blotch disease. The wheat spot blotch disease-causing fungus *Bipolaris sorokiniana* was effectively inhibited by the produced AgNPs. According to Vahabi et al.

(39), the inhibition of enzymes and toxins that fungal pathogens use for pathogenesis may be the cause of AgNPs antifungal efficacy. This demonstrates that the produced AgNPs are effective antifungal agents. AgNPs have found extensive use in the medical field, pharmaceutical sector, food preservation, wound care, dye reduction, antiseptic creams, textile coatings, and many environmental applications because of their antibacterial qualities (43,44,45).

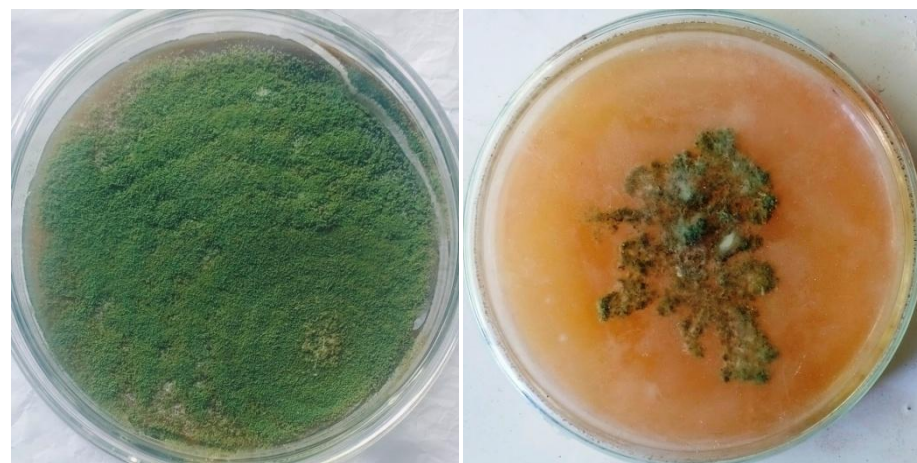


Figure 4. A- Untreated culture of *A. flavus*. B- Treated culture with AgNPs showing less growth.

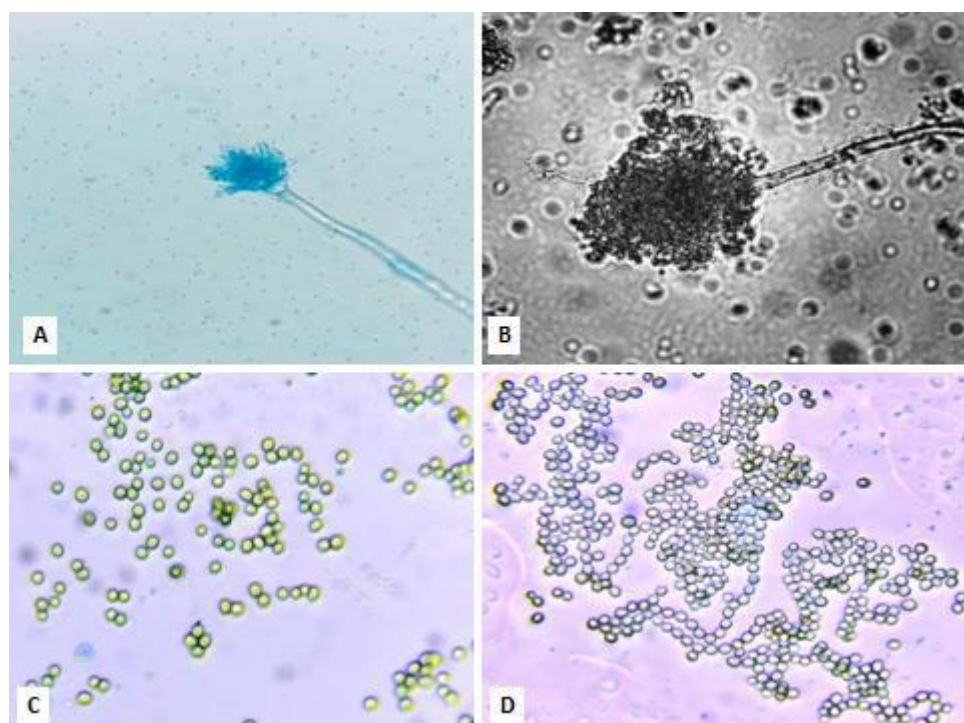


Figure 5. A- Conidia and Conidiophore under stereomicroscope stained with cotton blue and lactophenol B- Black and white Conidia and Conidiophore by Leica monochromatic microscope. C & D-Images showing fungal conidia of *A. flavus*

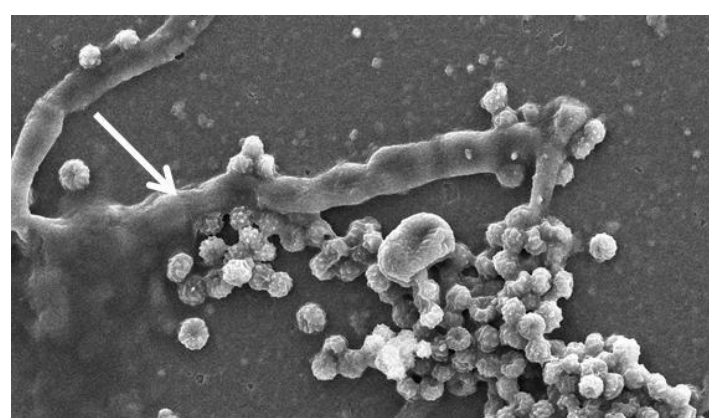


Figure 6. SEM image showing disturbed fungal mycelium treated with synthesized AgNPs



Figure 7. An inhibition zone around the wells filled with AgNPs (No inhibition zone around the untreated wells)

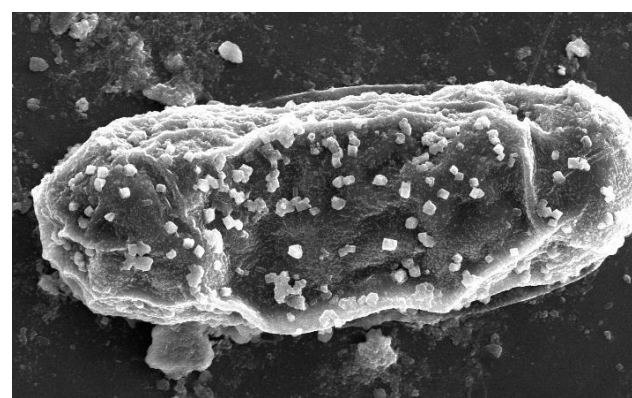


Figure 8. SEM image of bacteria treated with AgNPs

3.5. AgNPs effect on egg hatching and mortality under in vitro

AgNPs in water displayed lethal toxic effects upon direct contact with *M. incognita*. With longer exposure times, the effect becomes more pronounced. AgNPs inhibit eggs from hatching. In double-distilled water, maximum hatching occurred at 24 hours, 48 hours, and 72 hours (DDW). DD Water had the fewest dead nematodes after 24, 48, and 72 hours. Based on the application of AgNPs, egg hatching decreased with increasing time. Around 58% reduction in hatching has been reported after 72h. The synthesized AgNPs at 500 $\mu\text{g}/\text{ml}$ showed 6% J2 juvenile mortality after 24h, 16% after 48h, and 29% after 72h (Figure 9,10, 11).

In previous studies nematicidal effect of AgNPs also reported, Examination of the nematicidal properties of silver nanoparticles (AgNPs) made from *Conyza dioscoridis*, *Melia azedarach*, and *Moringa oleifera* leaf extracts was observed and findings showed that *C. dioscoridis* extractive silver nanoparticles had strong nematoidal activity against *Meloidogyne incognita* eggs and second stage juveniles (J2). Additionally, the nematicidal impact of AgNPs was comparable to that of rugby, the reference nematicide. The formulation of AgNPs increased several metabolites, as determined by the GC-MS study. Bis-(2-ethylhexyl)phthalate, β -isocomene, caryophyllene, β - and α -selinene, α -cadinol, berkheyaradulen, 6-epi-shyobunol, 4-hexylacetophenone, 1-hydroxy-1,7-dimethyl-4-isopropyl-2,7-cyclodecadiene, and aromadendrene were higher in AgNPs (40). In another study, silver nanoparticles were synthesized using the latex extract of *Euphorbia tirucalli* and screened against the root-knot nematode species *M. incognita*. AgNPs were found lethal to J2 and also inhibited egg hatching (*in-vitro*). *In-planta* trials suggest that infestation of *M. incognita* on tomato roots was significantly reduced when the AgNPs were applied as a root dip treatment (41). The AgNPs (100 $\mu\text{g}/\text{ml}$) synthesized from *Acalypha wilkesiana* showed 53.3% of nematode mortality (42).

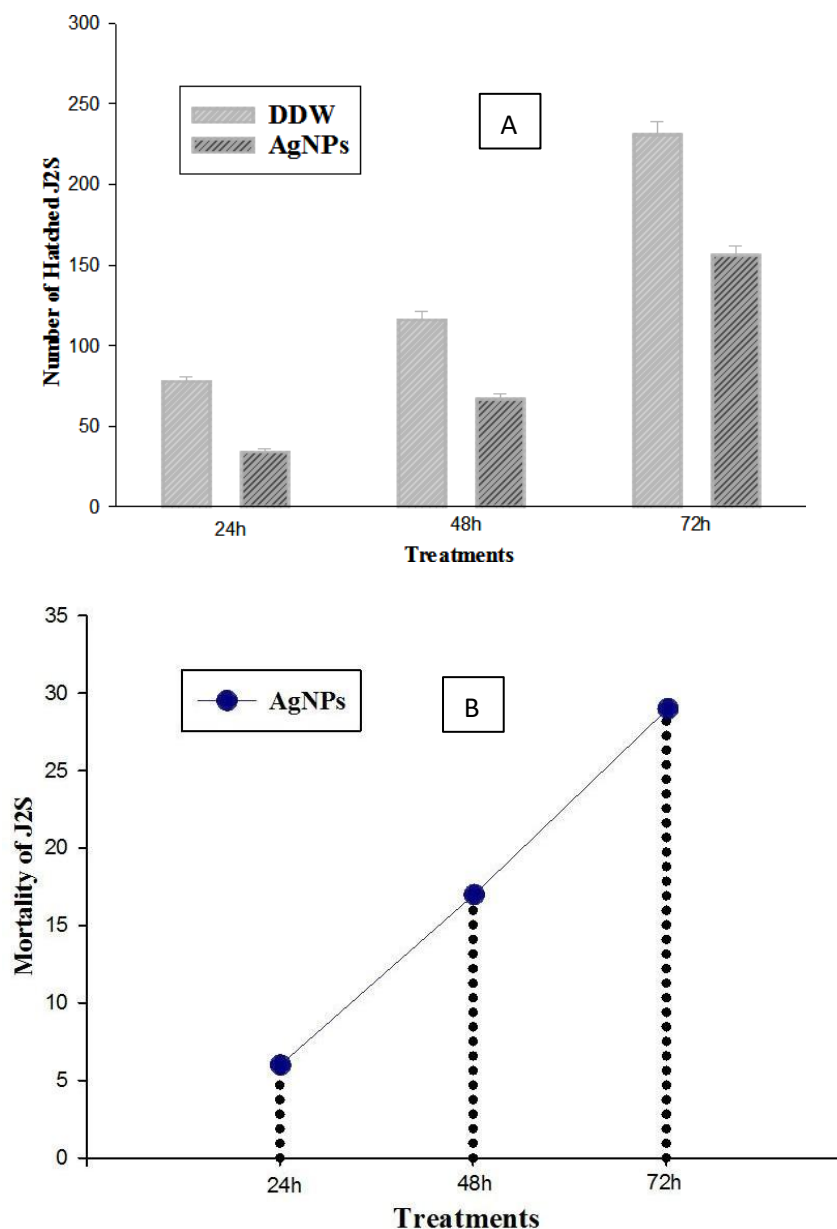


Figure 9. Effects of AgNPs on egg hatching and J2 juvenile viability of *M. incognita*. The eggs or J2s of *M. incognita* were incubated with a suspension of AgNPs in petri dishes. (A) The number of hatched juveniles was measured to count the rates of egg hatching after 24h, 48h, and 72h of incubation. (B) The mortality of J2 *M. incognita* was measured after 24h, 48 h, and 72h of incubation. DW, distilled water control.



Figure 10. A- Untreated Egg. B- Treated eggs of *M. incognita*

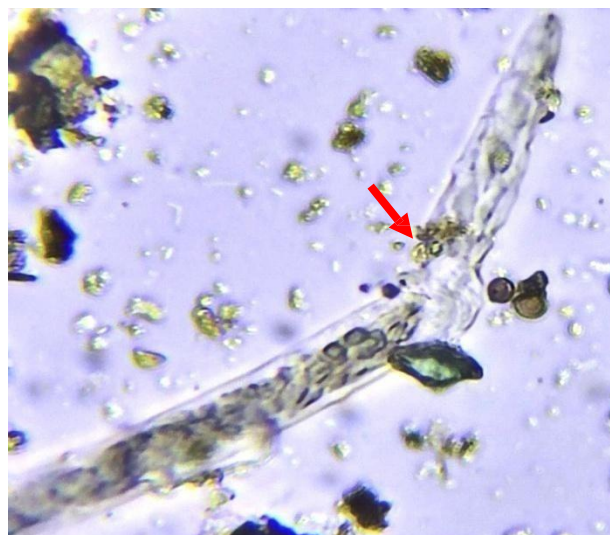


Figure 11. AgNPs treated J2 of *M. incognita* have a distorted body

4. Conclusions

This study described a straightforward biological synthesis of stable AgNPs at room temperature using plant extract. This is a safe, low-cost, clean, and environmentally friendly way to synthesize AgNPs. The synthesis and well-dispersed nature of the AgNPs were validated by the UV-visible spectroscopic, SEM, TEM, and FTIR techniques. AgNPs showed antifungal property against *A. flavus*, antibacterial property against *M. tuberculosis* and nematicidal property against *M. incognita*. Therefore, the biosynthesized AgNPs can be applied as an antibacterial agent to enhance agricultural productivity and ensure food safety and security. Given that the synthesized AgNPs have promising antifungal and nematicidal activities, further research can focus on optimizing the synthesis process to enhance bioactivity and reduce potential cytotoxicity. Collaboration with agricultural science and nanotechnology researchers can help scale up the production of these nanoparticles for practical applications in crop protection. Additionally, field trials evaluating the long-term efficacy and environmental impact of these AgNPs can promote their use as environmentally friendly alternatives for pest and disease management. Although some studies propose several mechanisms for AgNPs activity, including membrane rupture, DNA disruption, and reactive oxygen species (ROS), the mechanism is not entirely clear for the particular microbe under study. However, a thorough analysis is necessary to comprehend the intricate mechanisms behind AgNPs antifungal effect. Biogenic AgNPs have the potential to be employed to boost agricultural production, according to the results presented in this article. Before AgNPs are produced in large quantities and used in agriculture, more studies and field testing should be done to ascertain their harmful effects.

Conflict of Interest

The authors declare that they have no conflict of interest.

Reference

1. Gilbertson, L. M.; Pourzahedi, L.; Laughton, S.; Gao, X.; Zimmerman, J. B.; Theis, T. L.; Westerhoff, P.; Lowry, G.V. Guiding the design space for nanotechnology to advance sustainable crop production. *Nature nanotechnology*, **2020**, 15(9), 801-810.
2. *World Fertilizer Trends and Outlook to 2020: Summary Report* (Food and Agriculture Organization of the United Nations, **2017**).
3. Doljanović, Ž.; Nikolić, S.R.; Dragicevic, V.; Mutić, J.; Šeremešić, S.; Jovović, Z.; Popović D.J. Mineral composition of soil and the wheat grain in intensive and conservation cropping systems. *Agronomy*. **2022**, 12(6), 1321. <https://doi.org/10.3390/agronomy12061321>
4. Khan, M.; Popović-Djordjević, J.; Stanković, J.K. Nanomaterials as Effective Fertilizers and Fungicides in Plant Protection for Improving Crop Growth and Inducing Tolerance Against Phytopathogens. In *Nanoparticles in Plant Biotic Stress Management* (pp. 433-449). **2024**, Singapore: Springer Nature Singapore.
5. Alshahrani, A. A.; Alqarni, L. S.; Alghamdi, M. D.; Alotaibi, N. F.; Moustafa, S. M.; & Nassar, A. M. Photsynthesis via wasted onion peel extract of samarium oxide/silver core/shell nanoparticles for excellent inhibition of microbes. *Heliyon*, **2024**, 10(3).
6. Alqarni, L. S.; Alghamdi, M. D.; Alshahrani, A. A.; Alotaibi, N. F.; Moustafa, S. M.; Ashammari, K., ... & Nassar, A. M. Photocatalytic degradation of rhodamine-B and water densification via eco-friendly synthesized Cr₂O₃ and Ag@Cr₂O₃ using garlic peel aqueous extract. *Nanomaterials*, **2024**, 14(3), 289.
7. Khan, M.; Khan, A. U.; Moon, I. S.; Felimban, R.; Alserihi, R.; Alsanie, W.F.; Alam, M. Synthesis of biogenic silver nanoparticles from the seed coat waste of pistachio (*Pistacia vera*) and their effect on the growth of eggplant. *Nanotechnology Reviews*, **2021**, 10(1), 1789-800.

8. Worrall, E. A.; Hamid, A.; Mody, K. T.; Mitter, N.; Pappu, H.R. Nanotechnology for plant disease management. *Agronomy*, **2018**, 8(12), p.285.
9. Shakeel, Q.; Lyu, A.; Zhang, J.; Wu, M.; Li, G.; Hsiang, T.; Yang, L. Biocontrol of *Aspergillus flavus* on peanut kernels using *Streptomyces yanglinensis* 3–10. *Front. Microbiol.* **2018**, 9, 1049.
10. Amaike, S.; Keller, N.P. *Aspergillus flavus*. *Annu. Rev. Phytopathol.* **2011**, 8, 107–133.
11. Khan, M.; Khan, A.U. Plant parasitic nematodes effectors and their crosstalk with defense response of host plants: A battle underground. *Rhizosphere*, **2021**, 17, 100288
12. Khan, M.; Siddiqui, Z.A. Interaction of *Meloidogyne incognita*, *Ralstonia solanacearum* and *Phomopsis vexans* eggplant in the sand mix and fly ash mix soils. *Scientia Horticulturae*, **2017**, 225, 177–184.
13. Moradi R. M.; Pourakbar L.; Moghaddam S. S.; Popović-Djordjević J. The impact of TiO₂ nanoparticles on growth, chemical and antioxidant traits of saffron (*Crocus sativus* L.) exposed to UV-B stress. *Industrial Crops and Products*, **2019**, 137, 137–143.
14. Narware, J.; Singh, S.P.; Manzar, N.; Kashyap, A.S. Biogenic synthesis, characterization, and evaluation of synthesized nanoparticles against the pathogenic fungus *Alternaria solani*. *Frontiers in Microbiology*, **2023**, 14, p.1159251.
15. Durán, N.; Marcato, P. D.; Alves, O. L.; Souza, G.; Esposito, E. Mechanistic aspects of biosynthesis of silver nanoparticles by several *Fusarium oxysporum* strains. *J. Nanobiotechnol.*, **2005**, 3, 1–8.
16. Khan, A. U.; Malik, N.; Khan, M.; Cho, Khan, M. H. Fungi-assisted silver nanoparticles synthesis and their applications. *Bioprocess Biosystem Engineering*, **2018**, 41, 1-20 .
17. Khan, M.; Khan, A.U.; Rafatullah, M.; M. Alam, N. Bogdanchikova and D. Garibo Search for Effective Approaches to Fight Microorganisms Causing High Losses in Agriculture: Application of *P. lilacinum*Metabolites and Mycosynthesised Silver Nanoparticles. *Biomolecules*, **2022**, 12, 174.
18. Tidke, P. R.; Gupta, I.; Gade, A. K.; Rai, M. Fungus-mediated synthesis of gold nanoparticles and standardization of parameters for its biosynthesis, IEEE Trans Nanobioscience. **2014**, 13(4), 397–402.
19. Emeka,E. E.; Ojiefoh, O. C.; Aleruchi, C. Evaluation of antibacterial activities of silver nanoparticles green-synthesized using pineapple leaf (*Ananas comosus*). *Micron*. **2014**, 57, 1–5.
20. Kim, Y. S.; Kim, J. S.; Cho, H. S.; Rha, D. S.; Kim, J. M.; Park, J. D.; Choi, B.S.; Lim, R.; Chang, H. K.; Chung, Y. H.; Kwon, I. H., Jeong, J.; Han, B.S. Yu, I.J. Twenty-eight day oral toxicity, genotoxicity, and gender-related issue distribution of silver nanoparticles in Sprague-Dawley rats, *Inhal. Toxicol.* **2008**, 20, 575–583.
21. Jeong,S. H.; Yeo,S. Y.; Yi, S.C. The effect of filler particle size on the antibacterial properties of compounded polymer/silver fibers. *J. Mater. Sci.* **2005**, 40(20), 5407–5411
22. Parveen, A.; Siddiqui, Z. A. Effect of Silver Oxide Nanoparticles on Growth, Activities of Defense Enzymes and Fungal and Bacterial Diseases of tomato. *Gesunde Pflanzen*, **2023**, 75(2), 405-14.
23. Dasila, K.; Singh, M., Bioactive compounds and biological activities of *Elaeagnus latifolia* L.: an underutilized fruit of North-East Himalaya, India. *South African Journal of Botany*, **2022**, 145, 177-185.
24. Khan, A. U.; Khan, M.; Khan, M.M. Antifungal and Antibacterial Assay by Silver Nanoparticles Synthesized from Aqueous Leaf Extract of *Trigonella foenum-graecum*. *BioNanoScience*, **2019**, 9, 597-605.
25. Khan, M.; Khan, A. U.; Alam, M. J.; Park,S.; Alam, M. Biosynthesis of silver nanoparticles and its application against phytopathogenic bacterium and fungus. *J. Environ. Anal. Chem.* **2020**, 100(12), 1390-1401.
26. Varghese, R.; Almalki, M.A.; Ilavenil, S.; Rebecca, J.; Choi, K.C. Silver nanopaticles synthesized using the seed extract of *Trigonella foenum-graecum* L. and their antimicrobial mechanism and anticancer properties. *Saudi J. Biol. Sci.*, **2019**, 26(1), 148–154.
27. Alqarni, L. S.; Algamdi, M. D.; Alshahrani, A. A.; Nassar, A.M. Green nanotechnology: Recent research on bioresource-based nanoparticle synthesis and applications. *Journal of Chemistry*, **2022**, (1), 4030999.
28. Thao, T. T. P.; Luu, N. T.; Chi, N. L.; Hau, V. T. B.; Thuy, N. T. T. The first phytochemical study of *Elaeagnus latifolia* in Vietnsam. *Vietnam Journal of Chemistry*, **2021**, 59(3), 376-382.
29. MecoZZi, M.; Pietroletti, M.; Scarpiniti, M.; Acquistucci, R.; Conti, M.E. Monitoring of marine mucilage formation in Italian seas investigated by infrared spectroscopy and independent component analysis. *Environ. Monit. Assess.* **2012**, 184, 6025–6036.
30. Kumar, K., J.; Devi Prasad, A.G. Identification and comparison of biomolecules in medicinal plants of *Tephrosia tinctoria* and *Atylosia albicans* by using FTIR. *Rom. J. Biophys.* **2011**, 21, 63–71.
31. MecoZZi, M.; Sturchio, E. Computer Assisted Examination of Infrared and Near Infrared Spectra to Assess Structural and Molecular Changes in Biological Samples Exposed to Pollutants: A Case of Study. *J. Imaging* **2017**, 3, 11.
32. Zhang, Q.; Zhang, S.; Zhu, R.; Qiu, S.; Wu, Y. Synergistic Effect Between Fat Coal and Poplar During Co-Pyrolysis with Thermal Behavior and ATR-FTIR Analysis. In *Energy Technology 2018*; Sun, Z.; Wang, C.; Guillen, D.P.; Neelamegham, N.R., Zhang, L., Howarter, J.A., Wang, T., Olivetti, E., Zhang, M., Verhulst, D.; et al., Eds.; TMS 2018; The Minerals, Metals & Materials Series; Springer: Cham, Switzerland, 2018.
33. Khan, M.; Khan, A. U.; Bogdanchikova, N.; Garibo, D. Antibacterial and Antifungal Studies of Biosynthesized Silver Nanoparticles against Plant Parasitic Nematode *Meloidogyne incognita*, Plant Pathogens *Ralstonia solanacearum* and *Fusarium oxysporum*. *Molecules*, **2021**, 26, 2462.
34. Bocate, K. P.; Reis, G. F.; de Souza, P. C.; Junior, A. G. O.; Durán, N., Nakazato, G., ... & Panagio, L.A. Antifungal activity of silver nanoparticles and simvastatin against toxigenic species of *Aspergillus*. *Int. J. Food Microbiol.* **2019**, 291, 79-86.

35. Bahrami-Teimoori, B.; Nikparast, Y.; Hojatianfar, M.; Akhlaghi, M., Ghorbani, R., & Pourianfar, H. R. Characterisation and antifungal activity of silver nanoparticles biologically synthesised by Amaranthus retroflexus leaf extract. *Journal of Experimental Nanoscience*, **2017**, 12(1), 129-139.
36. Woo, K.S.; Kim, K.S.; Lamsal, K. et al. An *in vitro* study of the anti-fungal effect of silver nanoparticles on oak wilt pathogen *Raffaelea sp.*, *J. Microbiol Biotechnol*. **2009**, 19(8), 760–764.
37. Alotaibi, N. F.; ALqarni, L. S.; Alghamdi, S. Q.; Al-Ghamdi, S. N.; Amna, T.; Alzahrani, S. S., ... & Nassar, A. M. Green Synthesis of Uncoated and Olive Leaf Extract-Coated Silver Nanoparticles: Sunlight Photocatalytic, Antiparasitic, and Antifungal Activities. *International Journal of Molecular Sciences*, **2024**, 25(6), 3082.
38. Mishra, S.; Singh, B.R.; Singh, A. Biofabricated silver nanoparticles act as a strong fungicide against *Bipolaris sorokiniana* causing Spot Blotch disease in wheat. *PLoS One*, **2014**, 9(5), 978-81.
39. Vahabi, K.; Mansoori, G.A.; Karimi, S. Biosynthesis of silver nanoparticles by fungus *Trichoderma Reesei*. *Inscience J.* **2011**, 1, 65-79.
40. Abbassy, M. A.; Abdel-Rasoul, M. A.; Nassar, A. M.; & Soliman, B. S. Nematicidal activity of silver nanoparticles of botanical products against root-knot nematode, *Meloidogyne incognita*. *Archives of Phytopathology and Plant Protection*, **2017**, 50(17-18), 909-926.
41. Kalaiselvi, D.; Mohankumar, A.; Shanmugam, G.; Nivitha, S.; Sundararaj, P. Green synthesis of silver nanoparticles using latex extract of *Euphorbia tirucalli*: a novel approach for the management of root knot nematode, *Meloidogyne incognita*. *Crop Protection*, **2019**, 117, 108-114.
42. Heflish, A. A.; Hanfy, A. E.; Ansari, M. J.; Dessoky, E. S.; Attia, A. O.; Elshaer, M. M., ... & Behiry, S.I. Green biosynthesized silver nanoparticles using *Acalypha wilkesiana* extract control root-knot nematode. *Journal of King Saud University-Science*, **2021**, 33(6), 101516.
43. Parmar, S.; Kaur, H.; Singh, J.; Matharu, A. S.; Ramakrishna, S.; Bechelany, M. Recent advances in green synthesis of Ag NPs for extenuating antimicrobial resistance. *Nanomaterials*, **2022**, 12(7), 1115.
44. Khan, T.; Rahman, Q. I.; Raza, S.; Zehra, S.; Ahmad, N.; Husen, A. Nanodimensional materials: an approach toward the biogenic synthesis. In *Advances in smart nanomaterials and their applications*, **2023**, (pp. 523-568). Elsevier.
45. Ullah, A.; Lim, S. I. Plant extract-based synthesis of metallic nanomaterials, their applications, and safety concerns. *Biotechnology and Bioengineering*, **2022**, 119(9), 2273-2304.